

Models of dynamic extraction of lipid tethers from cell membranes

Sarah A. Nowak

RAND Corporation, Los Angeles, CA 90405

Tom Chou

Dept. of Biomathematics, UCLA, Los Angeles, CA 90095-1766

Dept. of Mathematics, UCLA, Los Angeles, CA 90095-1555

Abstract.

When a ligand that is bound to an integral membrane receptor is pulled, the membrane and the underlying cytoskeleton can deform before either the membrane delaminates from the cytoskeleton or the ligand detaches from the receptor. If the membrane delaminates from the cytoskeleton, it may be further extruded and form a membrane tether. We develop a phenomenological model for this processes by assuming that deformations obey Hooke's law up to a critical force at which the cell membrane locally detaches from the cytoskeleton and a membrane tether forms. We compute the probability of tether formation and show that they can be extruded only within an intermediate range of force loading rates and pulling velocities. The mean tether length that arises at the moment of ligand detachment is computed as are the force loading rates and pulling velocities that yield the longest tethers.

E-mail: tomchou@ucla.edu

1. INTRODUCTION

Adhesion between cells plays an important role in a number of biological processes involving cell motility and cell-cell communication. Cell-cell adhesion is mediated by integral membrane proteins on the surfaces of interacting cells. Cadherins, which mediate binding between cells of the same type within a tissue, bind to themselves, while integrins, which mediate binding between different cell types bind to Inter-Cellular Adhesion Molecules (ICAMs) or Vascular Cell Adhesion Molecules (VCAMs) [1]. Understanding the physics of this adhesive interaction requires an understanding of both the protein-protein bond as well as the cell's mechanical response when these bonds become stressed. If forces act to pull the two cells apart, either of the cells' cytoskeletons and plasma membranes may deform. Under certain conditions, the lipid membranes can delaminate from the underlying cytoskeleton and be pulled into long tethers. At any time during this process, the bonds holding the two cells together may also break, arresting tether extraction.

A specific biological process in which bond dissociation and membrane deformation must be considered simultaneously is leukocyte extravasation, which is part of the process by which leukocytes are recruited to inflamed or infected tissue. Endothelial cells that make up blood vessels preferentially express cellular adhesion

molecules, including selectins, near wounded tissue. Leukocytes circulating in the blood can then bind to the endothelial cells via their own cell surface proteins. Bonds between the leukocytes and the endothelial tissue are transiently made and broken as a shear flow in the blood vessel pushes the leukocyte, rolling it across the endothelial layer [2]. The rolling leukocytes contain microvilli that are enriched in adhesion molecules that preferentially attach to endothelial cells. During rolling, these microvilli tethers can extend under the hydrodynamic shear force of blood flow in the vessel [3]. At the same time, forces imposed on the endothelial membrane via the adhesion molecule can cause the endothelial membrane to form a tether [4]. Tether formation and extension of microvilli can decrease the force that the adhesive bond feels from the shear blood flow.

Both the physics of cell membrane deformation and the mechanics of ligand-receptor bonds have been studied extensively. Micropipette, atomic force microscope (AFM), optical trap, and magnetic bead techniques have been used to pull membrane tethers from cells and probe the properties of the cell membrane [5]. The diameter of the extracted tether depends on the membrane surface tension and bending rigidity and, if the tether is being extended at a constant velocity, the membrane viscosity [6, 7]. Therefore, these quantities can be inferred from tether pulling or poking experiments [8]. Theoretically, Euler-Lagrange methods have been used to compute equilibrium tether shapes and the force-extension curve for a tether pulled quasi-statically from a lipid vesicle [9, 10]. These theoretical models of pure lipid bilayers show only a $\sim 10\%$ overshoot, or barrier, in the force-extension curve before a tether is extracted from an asymptotically flat membrane [9, 10]†, some experiments show a significant force barrier to tether formation [11, 12, 13]. These large force barriers to membrane tether formation arise in living cells and is attributed to membrane adhesion to the underlying actin cytoskeleton [11, 14]. When tethers are pulled from giant artificial vesicles, the size of the force barrier can increase only when the area on which the pulling force is exerted is increased [12]. For smaller vesicles, area and volume constraints may also influence the tether force-extension relationship [15]. These may arise from nonlocal terms in the functional describing the lipid membrane energetics. For example, area-difference elasticity can give rise to a restoring forces that continually increase as tether length increases [16, 17]. Such nonlocal effects will be important only when the tether comprises an appreciable fraction of the total membrane area. Force curves that do not saturate at long tether extensions can also arise when part of the membrane reservoir adheres to a substrate [13]. The relative importance of nonequilibrium forces arising from the viscosity of both the membrane lipids and surrounding solution have also been estimated [18].

During tether pulling experiments, and in their corresponding theoretical models, the molecular bond attaching the pulling device to the membrane is assumed to always remain intact. However, a typical ligand-receptor bond used to connect the pulling device to the lipid membrane (and possibly the underlying cytoskeleton) can rupture upon pulling. Although the details of a bond's energy landscape can be probed using dynamic force spectroscopy [19, 20, 21, 22], one can usually assume that bond rupturing is dominated by a single activation barrier that can be lowered by an externally applied pulling force. Most AFM studies of molecular strength are performed on proteins that have been isolated from cells. However, recent

† The barrier represents the energy that must be overcome before a lipid tether can be drawn out. The $\sim 10\%$ energy barrier arises from the Helfrich free-energy-minimizing geometry of an incipient lipid membrane tether in the absence any cytoskeletal attachments [9, 10] (cf. dashed curve in Fig. 2

studies have probed bond strengths between proteins still embedded in a live cell membrane [23, 24]. While using live cells has the advantage that the post-translational modifications of membrane proteins are preserved, the mechanical deformation of the cell's cytoskeleton and membrane must also be taken into account. To model this system, a viscoelastic Kelvin model was used to fit experimental measurements of the force-extension relationship to determine effective cellular adhesion [24].

In this paper, we develop a dynamic model that incorporates phenomenological theories of membrane and cytoskeleton deformation, tether extraction, and the kinetics of ligand-receptor detachment. In contrast to an equilibrium model determining tether extraction and detachment from an adhered vesicle [15], we find relationships that define when tether extraction is likely, and the typical length of the tether pulled before the ligand-receptor bond ruptures. In the next section, we motivate a simple mechanical model using phenomenological forms for the force-extension relationship of the membrane. Given the large bending energies of lipid bilayer membranes, and the relatively strong attachment of membranes to cytoskeleton, we will neglect thermal fluctuations of the membrane, but implicitly include thermally-driven ligand-receptor bond dissociation. Dynamical equations are written for two commonly employed experimental protocols, a linear force loading rate, and a constant bond pulling speed. In the Results and Discussion, we compute the probability of tether formation and plot universal curves that delineate regimes where tethers are likely to form. Mean tether lengths are also plotted for both pulling protocols.

2. Mathematical Model

Consider the system depicted in Figure 1. A ligand is bound to an integral membrane protein, which may also be directly associated with the cytoskeleton. The ligand may be attached to a pulling device via a cantilever spring and is pulled with either a fixed speed, or a force that increases linearly in time.

As the ligand is pulled, the cytoskeleton first deforms, and eventually can detach from the membrane. At this point, the lipid membrane may flow into a tether. At any point during the cytoskeletal or membrane deformation, before or after membrane-cytoskeleton delamination and tether formation, the ligand affixed to the pulling device may detach from the membrane receptor protein.

2.1. Membrane Mechanics

We first consider the response of the membrane-cytoskeleton system to an externally applied pulling force $F_p(t)$. The rate at which the receptor-ligand complex moves will be described by

$$\frac{dx(t)}{dt} = -\xi \left[\left. \frac{\partial U(x)}{\partial x} \right|_{x=x(t)} - F_p(t) \right] \quad (1)$$

where ξ is a mobility that is inversely related to the viscosity of the membrane lipid [18]. In general, although ξ depends on the configuration of the system defined predominantly by $x(t)$, we neglect the details of this dependence and assume it to be constant.

The term $U(x)$ represents the energetic cost associated with deforming the cell membrane and underlying cytoskeleton when the receptor is displaced a distance x normal to the flat membrane. This phenomenological energy can be derived from

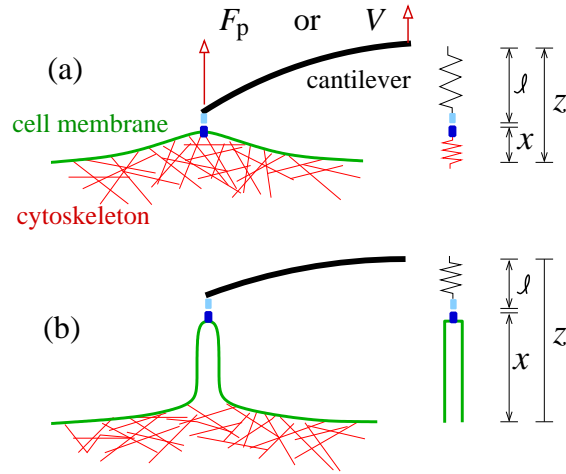


Figure 1. (a) A cell membrane can be pulled by a device such as a cantilever. The device can be moved at fixed velocity V , or, at a specified force $F_p(t)$. Under specified force conditions, the transduction of force through the device is assumed instantaneous such that $F_p(t)$ is always acting across the ligand-receptor bond. Before membrane delamination from the underlying cytoskeleton, the pulling results in small membrane and cytoskeletal deformations. (b) After membrane delamination, the pulling device can extrude long lipid tethers without deforming the cytoskeleton. The total system length z is the sum of the displacement x of the membrane protein from its initial position and ℓ , the increase in the length of the cantilever spring from its unstretched length.

a detailed consideration of the membrane-cytoskeletal mechanics. For simplicity, we will assume the membrane mechanics are governed by a Helfrich free-energy [25] that includes a lipid bilayer bending rigidity and an effective thermally-derived entropic membrane tension. We will assume that the membrane reservoir is large enough such that an extruded tether negligibly depletes the reservoir. Hence, global contributions to the membrane energetics, such as area-difference elasticity, can be neglected.

Experiments in which tethers were pulled from live cells found a significant force barrier to tether formation [11, 14]. While a smaller force barrier can also arise in pure lipid membranes [9], we will assume that the plasma membrane is attached to an underlying cytoskeleton (with anchoring molecules), which we model as a linear elastic material provided the deformation is small. The receptor that binds the ligand that is attached to the pulling device can also be a transmembrane receptor that is directly attached to the cytoskeleton. As the membrane is initially pulled, the cytoskeleton will elastically deform as a Hookean spring. The receptor or anchoring molecules will break at a deformation x_0 , and the lipid membrane will be drawn into a tether. This occurs at a critical delamination force F_c . Thus, for displacements $x < x_0$, where the Hookean approximation for the membrane-cytoskeleton assembly is valid, the membrane-cytoskeleton carries an effective spring constant F_c/x_0 , where F_c is the critical delamination force. Experimentally, the cytoskeleton typically detaches from the membrane where the filament-free tether forms [26, 27]; therefore we can assume a linear force extension relationship of the form

$$\frac{\partial U}{\partial x} = \frac{x}{x_0} F_c, \quad x < x_0. \quad (2)$$

At a displacement $x = x_0$, the membrane delaminates from the cytoskeleton and a lipid membrane tether forms. Under the infinite reservoir and simple Helfrich free-energy assumption, the tether can then elongate indefinitely under a constant force $\partial U/\partial x = F_0$ that is intrinsic to the lipid tether and is determined by the membrane bending rigidity κ and entropic surface tension σ [9, 10]: $F_0 = 2\pi\sqrt{2\kappa\sigma}$. The phenomenological membrane force-displacement relationship for both attached

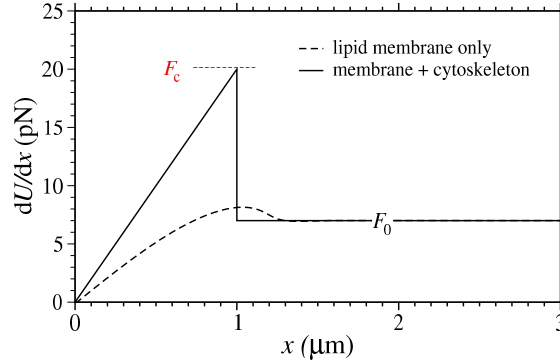


Figure 2. We assume that when the receptor is initially associated with the cytoskeleton, $\partial_x U(x)$ increases linearly until some maximum force F_c in the barrier to tether formation is reached, after which the tether extends with constant force F_0 (solid curve). The qualitative features of this force-extension curve is observed in numerous systems [7, 11, 12, 13, 14]. For reference, we show $\partial_x U(x)$ as a function of x when the only contributions to $U(x)$ come from membrane surface tension and bending rigidity (dashed curve). This curve was calculated using the method described in [9] assuming a membrane bending rigidity of $20k_B T$ and a surface tension of 0.0076 dynes/cm.

(solid curve) and free (dashed curve) membranes are shown in Figure 2. The barrier F_c to tether formation is larger for receptors or membranes that are attached to the underlying cytoskeleton, than for the free lipid membrane case.

In order to close the equations of our basic model, we must specify $F_p(t)$. Henceforth, we will consider two cases typically realized in experiments: a linearly increasing (in time) pulling force, and a fixed pulling speed.

2.2. Linear Force Ramp

For a force linearly increasing in time, $F_p(t) = \Gamma t$, where Γ is the rate with which the force increases. Eq. 1 becomes

$$\frac{dx(t)}{dt} = -\xi \left[\frac{\partial U(x)}{\partial x} - \Gamma t \right]. \quad (3)$$

Upon defining the time t_0 at which the membrane delaminates from the cytoskeleton provided the ligand-receptor bond has not yet ruptured by $x(t = t_0) \equiv x_0$, we have $\frac{\partial U}{\partial x} = (x/x_0)F_c$ for $t \leq t_0$, and $\frac{\partial U}{\partial x} = F_0$ for $t > t_0$. Thus, Eq. 3 is solved by

$$x(t < t_0) = \frac{x_0 \Gamma}{F_c} t - \frac{\Gamma x_0^2}{\xi F_c^2} (1 - e^{-\xi F_c t / x_0}), \quad (4)$$

and

$$x(t > t_0) = x_0 - \xi F_0(t - t_0) + \frac{\xi \Gamma}{2}(t^2 - t_0^2), \quad (5)$$

where the delamination t_0 is determined from the solution to

$$\frac{\Gamma}{F_c} t_0 - \frac{\Gamma x_0}{\xi F_c^2} (1 - e^{-\xi F_c t_0 / x_0}) = 1. \quad (6)$$

2.3. Constant Pulling Speed

In the case of constant pulling speed, we must include the dynamics of the device deformation $\ell(t)$. Since the velocity of the pulling device is fixed, we note that the total displacement $z(t) = x(t) + \ell(t)$ obeys

$$\frac{dz}{dt} = \frac{dx}{dt} + \frac{d\ell}{dt} = V. \quad (7)$$

This equation holds only when the ligand is attached to the membrane-bound receptor. Let us assume that the pulling device has an internal response that is modeled by a simple spring so that the force $F_p(t)$ that the spring exerts on the ligand is

$$F_p(t) = K\ell(t), \quad (8)$$

where K is the spring constant of the pulling device. Since the pulling force is proportional to $\ell(t)$, it will ultimately depend on the pulling rate V and the physical properties of the pulling device (represented by an elastic cantilever in Figure 1) and cell membrane through Eq. 7. Upon integrating Eq. 7 and using the initial conditions $x(t=0) = \ell(t=0) = 0$, we find

$$x(t) = Vt - \ell(t). \quad (9)$$

Substituting Eqs. 9 and 8 into Eq. 1, and expressing the dynamics in terms of the device deformation, we find a closed equation for $\ell(t)$:

$$\frac{d\ell}{dt} = V + \xi \left[\left. \frac{\partial U(x)}{\partial x} \right|_{x=Vt-\ell(t)} - K\ell(t) \right]. \quad (10)$$

This equation is solved by

$$\ell(t \leq t_0) = \frac{VKx_0^2}{\xi(F_c + Kx_0)^2} (1 - e^{-\xi(K+F_c/x_0)t}) + \frac{F_c V t}{F_c + Kx_0} \quad (11)$$

for $t < t_0$, and

$$\ell(t > t_0) = \frac{V + \xi F_0}{\xi K} (1 - e^{-\xi K(t-t_0)}) + \ell(t_0) e^{-\xi K(t-t_0)} \quad (12)$$

for $t > t_0$ (when $\partial U/\partial x = F_0$). Here, the time t_0 at which tether formation occurs is found by evaluating Eq. 9 at time $t = t_0$, $x(t_0) = x_0 = Vt_0 - \ell(t_0)$, yielding an implicit equation for t_0 :

$$Vt_0 - x_0 = \frac{F_c V t_0}{F_c + K x_0} + \frac{V K x_0^2}{\xi(F_c + K x_0)^2} (1 - e^{-\xi(K + F_c/x_0)t_0}). \quad (13)$$

After evaluating t_0 numerically, $\ell(t)$ is found in terms of the K , V , ξ , F_c , F_0 , and x_0 , and the membrane displacement can be found using Eq. 9.

2.4. Ligand-Receptor Dissociation

The dynamics described above for the membrane and pulling device deformations assume that the pulling device remains attached to the membrane through an unbroken ligand-receptor bond. Since all external forces are transduced through the ligand-receptor bond, the pulling force $F_p(t)$ on the membrane (cf. Eq. 1) vanishes once the ligand-receptor bond ruptures. However, the probability of ligand-receptor bond dissociation itself depends on the applied force $F_p(t)$. We can model the breaking of the ligand-receptor bond by a Poisson process and define a ligand-receptor bond survival probability $Q(t)$ that obeys

$$\frac{dQ(t)}{dt} = -k_r(t)Q(t), \quad (14)$$

where $k_r(t)$ is the force-dependent rupture (or dissociation) rate of the ligand from the receptor. We assume that $k_r(t)$ takes a simple Arrhenius form [28]:

$$k_r(t) = k_0 e^{F_p(t)d/k_B T}, \quad (15)$$

where d is the length of the ligand-receptor bond and $k_B T$ is the thermal energy. The solution to Eq. 14 is explicitly

$$Q(t) = \exp \left[-k_0 \int_0^t e^{F_p(t')d/k_B T} dt' \right]. \quad (16)$$

More complex models of dynamics bond rupturing can be derived [29, 30]. Here, for simplicity, molecular details such as the thermally-induced bond-breaking attempt frequency and the intrinsic free energy of the unstressed ligand-receptor bond are subsumed in the effective rate parameter k_0 .

Since $w(t) \equiv -dQ(t)/dt = k_r(t)Q(t)$ is the bond rupture time distribution, the mean membrane displacement at the time of ligand-receptor rupture (the mean maximum displacement) is given by

$$\langle x^* \rangle \equiv \int_0^\infty w(t)x(t)dt = \int_0^\infty k_r(t)Q(t)x(t)dt. \quad (17)$$

In our subsequent analysis, we will combine bond rupturing statistics with membrane tether dynamics and explore, as a function of the physical parameters, the probability of tether formation, and the length of pulled tethers should they form. To be concrete, we will use typical parameter values (listed in Table I) found from the relevant literature to guide our analysis.

parameter	range of values	reference
d	0.8-1.0 nm	[31] (streptavidin-HABA)
ξ	$\sim 1\mu\text{m}/(\text{pNs})$	[18]
x_0	$\sim 1 - 4\mu\text{m}$	[11]
F_0	3-380pN	calculated [‡]
F_c	100-380pN 1-100pN	[27] (red blood cells) [32] (epithelial cells)
K	8-11pN/ μm	[11]
k_0	10^{-5} -10/s	[33]
V	$\sim 3 \mu\text{m/s}$	[11]
Γ	10pN/s	[11]

3. Results

Here, we compute the dynamics of tether formation and ligand-receptor bond rupturing under both linear force loading and constant pulling velocity protocols.

3.1. Linear Force Ramp

When $F_p(t) = \Gamma t$, the ligand-receptor survival probability defined by Eq. 16 is explicitly

$$Q(t) = \exp \left[-\frac{k_0 k_B T}{\Gamma d} (e^{\Gamma t d / k_B T} - 1) \right], \quad (18)$$

The bond survival probability, evaluated at the time of tether formation t_0 (found numerically from Eq. 6), $Q(t_0) \equiv P_T$, determines the likelihood that a tether is extracted, and is plotted in Fig. 3(a) as a function of force loading rate Γ . Note that P_T first increases with the force loading rate Γ , before decreasing again at very high loading rates. Large critical delamination forces F_c increase the probability that ligand-receptor bonds detach before membrane-cytoskeleton delamination occurs. Membrane-cytoskeleton combinations that have weaker delamination forces F_c yield a larger range of force loading rates that lead to tether formation. Moreover, since the pulling force is specified, $Q(t)$ is independent of the free tether restoring force F_0 (cf. Eq. 18). The only dependence is on the delamination force F_c which sets the delamination t_0 (cf. Eq. 6) in the expression $P_T \equiv Q(t_0)$. Once the tether is formed, the free tether restoring force F_0 is irrelevant. The values Γ_+ and Γ_- are defined by $P_T(\Gamma_{\pm}) = 1/2$ and define the window of loading rates within which tether formation is likely.

For quantitative evaluation of Γ_{\pm} , and their dependences on the other system parameters (F_{\max} , d , $k_B T$, x_0 , and ξ), it is convenient to define dimensionless parameters according to

$$\gamma \equiv \frac{\xi \Gamma}{k_0^2 x_0}, \quad \alpha \equiv \frac{k_0 x_0 d}{\xi k_B T}, \quad f_c = \frac{\xi F_c}{k_0 x_0}, \quad (19)$$

and find parameter regimes within which $P_T \geq 1/2$. Upon using Eq. 18, the phase boundaries for tether formation are determined from the implicit solution to

$$\exp \left[-\frac{1}{\alpha \gamma} (e^{\alpha \gamma \tau_0(\gamma, f_c)} - 1) \right] = \frac{1}{2}, \quad (20)$$

[‡] $F_0 = 2\sqrt{2}\pi\sqrt{\kappa\sigma}$ where κ is the membrane bending rigidity and σ is the effective membrane surface tension[9]. We assumed $\sigma = 3 - 1200\text{pN}/\mu\text{m}$ [34] and $\kappa = 10 - 20k_B T$ [35]

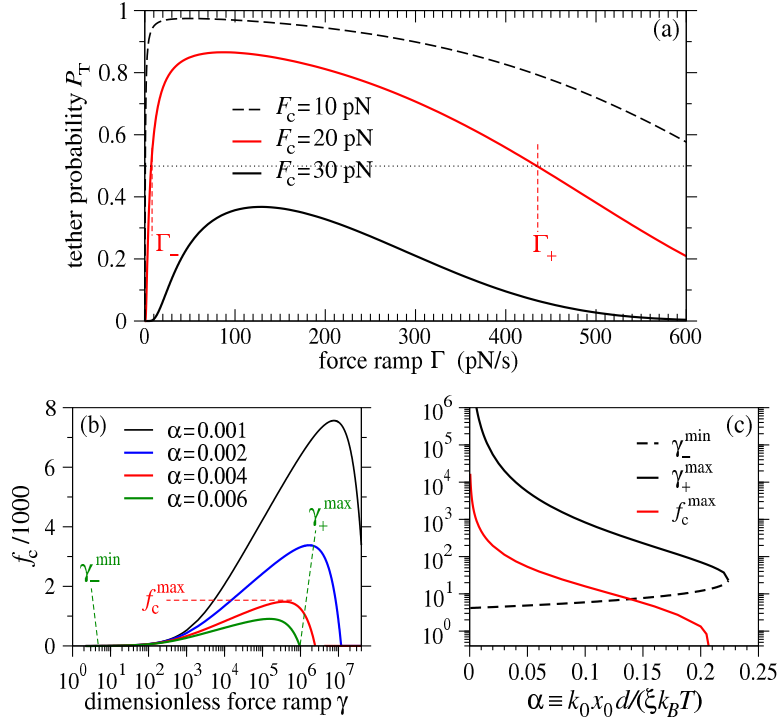


Figure 3. (a) Tether formation probability $P_T \equiv Q(t_0)$ as a function of force ramp rate Γ . Note that results for the constant force ramp protocol are independent of the free tether restoring force F_0 . Γ_{\pm} denote the linear loading rates at which the tether formation probability $P_T = 1/2$. Applied loading rates $\Gamma_- < \Gamma < \Gamma_+$ are likely to lead to tether formation. For $F_c = 20$ pN, $\Gamma_- \approx 7.2$ pN/s and $\Gamma_+ \approx 435$ pN/s. Other parameters used were: $k_0 = 0.01$ /s, $d = 1$ nm, $x_0 = 1$ μ m and $\xi = 1$ μ m/(pNs). (b) Dimensionless parameter regimes in which $P_T \geq 1/2$. The regions of parameter space below each curve are associated with $P_T > 1/2$, where tether formation is likely. The smaller the dimensionless bond dissociation rate $\alpha = k_0 x_0 d / (\xi k_B T)$, the wider the range of dimensionless loading rates $\gamma = \xi \Gamma / (k_0^2 x_0)$ leading to tether formation. The maximum and minimum pulling rates $\gamma_-^{\min} \equiv \gamma_-(f_c = 0)$ and $\gamma_+^{\max} \equiv \gamma_+(f_c = 0)$ are indicated for the $\alpha = 0.006$ curve, while the maximal dimensionless delamination force f_c^{\max} is shown for $\alpha = 0.004$. (c) The minimum and maximum force ramps, and the maxima delamination force as functions of α . For $\gamma < \gamma_-^{\min}$, $\gamma > \gamma_+^{\max}$, or $f_c > f_c^{\max}$, tethers *always* have less than 50% chance of forming.

where $\tau_0 = k_0 t_0$ is determined from the solution to the dimensionless form of Eq. 6:

$$\frac{\gamma \tau_0}{f_c} - \frac{\gamma}{f_c^2} (1 - e^{-f_c \tau_0}) = 1. \quad (21)$$

Figure 3(b) shows curves in dimensionless parameter space (f_c and γ) below which $P_T > 1/2$. Asymptotic analysis of the condition $P_T = 1/2$ shows that for sufficiently large γ , tether formation will always be suppressed. Additionally, as the dimensionless ligand-receptor dissociation rate α increases, the regime for tether formation shrinks.

Conditions for tether formation can be further refined by computing universal parameter curves that define regimes for which P_T can never be greater than 1/2. As a function of the intrinsic ligand-receptor dissociation rate, there is a band of pulling

rates outside of which P_T is always less than one half, even when tether extraction is barrierless ($f_c = 0$). Fig. 3(c) shows γ_-^{\min} and γ_+^{\max} , the minimum and maximum dimensionless ramp rates at which $P_T = 1/2$ when $f_c = 0$. These delimiting loading rates are roots of Eq. 20. For small α , the lower root $\gamma_-^{\max} \simeq 2/\ln^2 2 + O(\alpha)$.

Also plotted in Fig. 3(c) is $f_c^{\max}(\alpha)$, the maximum membrane-cytoskeleton delamination force that can give rise to $P_T \geq 1/2$, for any ramp rate. One is unlikely to pull tethers from membranes that require more force than f_c^{\max} to delaminate from the cytoskeleton. Moreover, there is a critical $\alpha^{\max} \approx 0.22444$ above which $P_T = 1/2$ cannot be reached, independent of f_c or γ .

Finally, we plot in Fig. 4 the expected dimensionless maximum tether length $\langle X^* \rangle \equiv \langle x^* \rangle / x_0$ found from Eq. 17, as a function of the dimensionless force loading rate γ . Not only does the mean tether length decrease with increasing critical

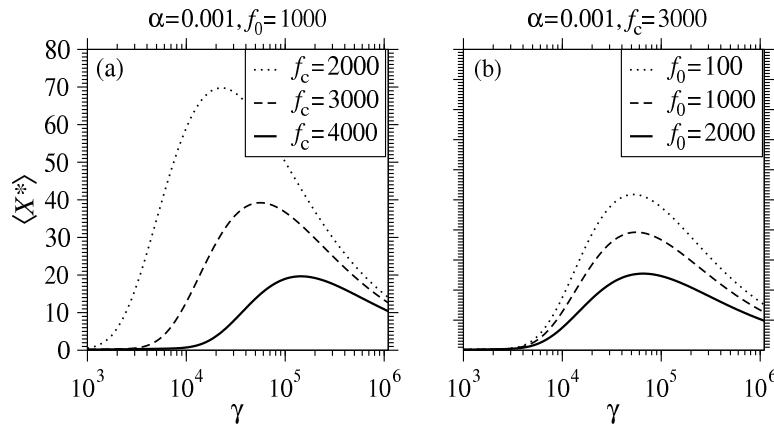


Figure 4. (a) Mean tether length $\langle X^* \rangle$ as a function of load rate γ for different critical delamination forces f_c . (b) $\langle X^* \rangle$ at fixed f_c and various f_0 . Even though the cytoskeleton-free membrane restoring force does not affect tether formation probability P_T , it does influence the length of tether possible.

delamination force f_c , as shown in Fig. 4(a), but the value of γ at which $\langle X^* \rangle$ is maximized decreases as f_c is raised. Since tether extrusion is a competition between the rate of climb against the restoring force $F_c x / x_0$ and ligand-receptor dissociation, as f_c is increased, higher ramp rates are required to cross the delamination barrier faster, relative to the bond rupturing. Although the free membrane restoring force $f_0 = \xi F_0 / (k_0 x_0)$ does not come into play in the tether formation probability, it does influence the mean length of lipid tether that is extruded before the ligand detaches from the membrane-bound receptor. Note that in the constant loading rate protocol, the force is specified and all results are independent of the pulling device rigidity K .

3.2. Constant Pulling Speed

Now consider a constant pulling speed protocol. The force felt by the membrane in this ensemble will depend on the pulling device rigidity K . The bond survival probability is computed from

$$Q(t) = \exp \left[-k_0 \int_0^t e^{K\ell(t')d/k_B T} dt' \right], \quad (22)$$

where $\ell(t)$ is given by Eqs. 11 and 12. Initially, while the membrane and cytoskeleton are attached to each other, and constant speed pulling is applied, the ligand-receptor bond survival probability $Q(t)$ first decreases rapidly. After delamination, the force on the ligand-receptor are fixed, arising only from F_0 and the viscous drag ξ^{-1} . The subsequent decay of $Q(t)$ arises from a slower, single exponential.

Fig. 5(a) shows the corresponding P_T as a function of pulling speed V , and as in the force ramp case, reveals an optimal pulling speed that maximizes the likelihood of pulling a tether. In the $V \rightarrow 0$ limit $x(t) \approx 0$ (from Eqs. 9 and 12), and we expect $P_T \rightarrow 0$ because when the ligand-receptor bond detaches, the membrane has not been sufficiently deformed. In the fast pulling limit, the detachment rate increases quickly and ligands detach at very short times t such that tether formation cannot occur. Upon defining $P_T(V_{\pm}) = 1/2$, pulling speeds $V_- < V < V_+$ are likely to result in tethers.

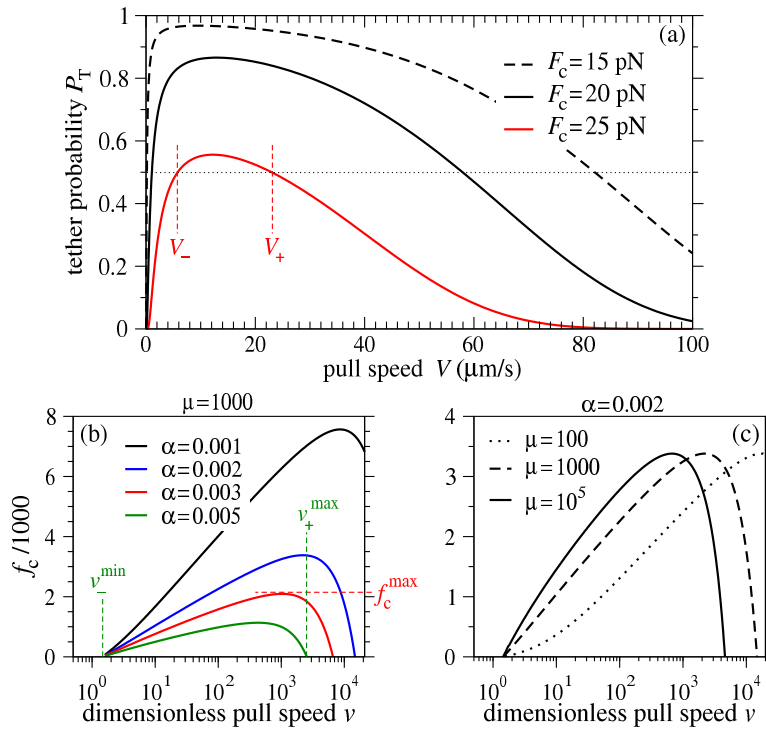


Figure 5. (a) The probability P_T that tether formation occurs before the ligand detaches from the receptor plotted as a function of pulling speed V . Analogous to the force ramp protocol, there is a band of pulling speeds $V_- < V < V_+$ within which the tether formation probability is greatest. Parameters used were: $k_0 = 0.01/\text{s}$, $d = 1\text{nm}$, $\xi = 1\mu\text{m}/(\text{pN s})$, $F_c = 20\text{pN}$, $K = 10\text{pN}/\mu\text{m}$. (b) Phase diagram in the $f_c = \xi F_c / (k_0 x_0)$ and $v = V / (k_0 x_0)$ parameter space for various $\alpha = k_0 x_0 d / (k_B T)$ and fixed pulling device stiffness $\mu = \xi K / k_0 = 1000$. (c) Phase diagram for fixed $\alpha = 0.002$ and various pulling device stiffnesses μ .

To explore how V_{\pm} depends on other system parameters, we employ the same dimensionless parameters defined in Eqs. 19, along with a dimensionless pulling speed

and pulling device stiffness,

$$v \equiv \frac{V}{k_0 x_0} \quad \text{and} \quad \mu \equiv \frac{K\xi}{k_0}. \quad (23)$$

Figure 5(b) shows, for $\mu = 1000$ and various values of α , the boundaries below which tether formation is likely. Fig. 5(c) shows the phase boundaries for fixed $\alpha = 0.002$ and various pulling device stiffnesses μ . Note that softer pulling devices suppress tether formation at low speeds since the forces are not immediately felt by the membrane, allowing the ligand more time to detach. However, softer pulling devices greatly enhance tether formation at large pull speeds because the accelerated delamination more than compensates for the drag-mediated acceleration of ligand-receptor dissociation.

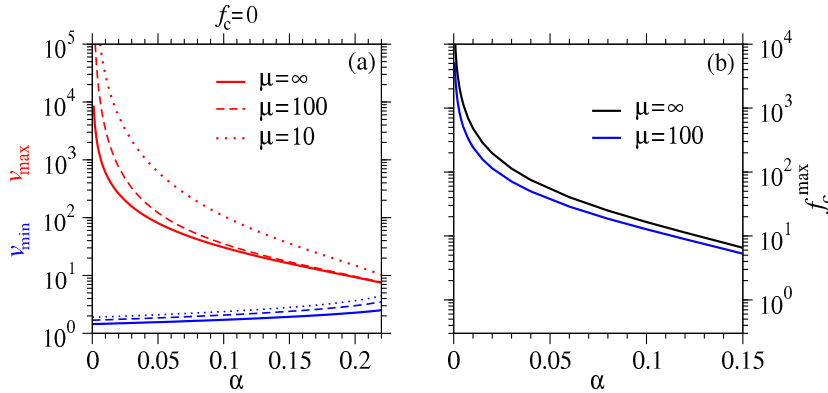


Figure 6. (a) Universal curves for the critical values v_{-}^{\min} and v_{+}^{\max} as a function of dimensionless unstressed ligand-receptor dissociation rate α . Curves for three different values of device stiffness μ are shown. For $\alpha \ll 1$ and $\mu \rightarrow \infty$, the minimum pull speed is asymptotically $v_{-}^{\min} \simeq 1/(\ln 2 - \alpha)$. In this limit, the critical α^{\max} beyond which v_{-}^{\min} and v_{+}^{\max} merge (and tether formation is unlikely, even for $f_c = 0$) occurs at $\alpha^{\max} \approx 0.24$, slightly larger than the α^{\max} in the constant load rate protocol (not shown). (b) The maximal delamination force f_c^{\max} as a function of α for two different stiffnesses μ .

Note that analogous to the linear force ramp protocol, for particular α and μ , there is a maximum and minimum pulling speed (v_{-}^{\min} and v_{+}^{\max}) beyond which tether formation is unlikely, even when the delamination force vanishes (Fig. 6(a)). Conversely, there is a maximum delamination force f_c^{\max} above which no pulling speed will result in likely tether formation (Fig. 6(b)).

Finally, consider the mean receptor displacement at the moment of ligand detachment, $\langle X^* \rangle \equiv \langle x^* \rangle / x_0$, found from Eq. 17 with $X(t) = v\tau - \ell(t)/x_0$, and the appropriate $Q(t)$ and $k_r(t)$. The same arguments that explain the non-monotonic behavior of P_T as a function of V apply here, and the mean dimensionless receptor displacement at the moment of ligand detachment, $\langle X^* \rangle$, is a non-monotonic function of V (Fig. 7). When the pulling velocity is small, the receptor moves slowly and the term $x(t)$ in Eq. 17 will be small, rendering integral in Eq. 17 small. On the other hand, when V is sufficiently large, the viscosity ξ^{-1} allows a large force to be reached, accelerating ligand-receptor bond rupturing. Thus, $Q(t)$ quickly decreases and the mean receptor displacement when the ligand detaches, $\langle x^* \rangle$, will be small.

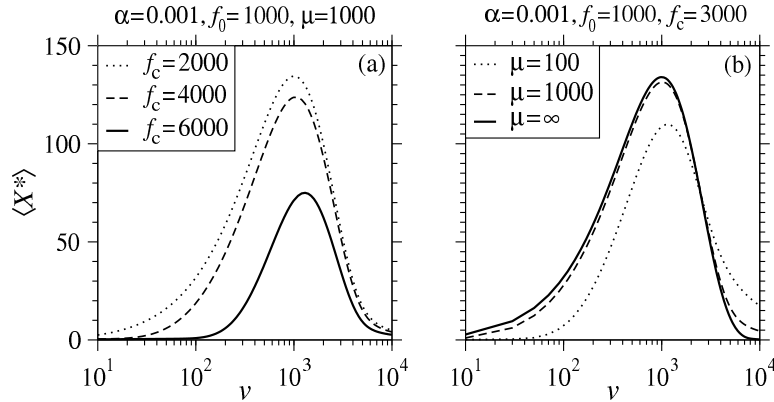


Figure 7. (a) The mean system length at ligand detachment, $\langle X^* \rangle$, is a non-monotonic function of the dimensionless pulling velocity, v , and increases with decreasing f_c . The qualitative dependence of $\langle X^* \rangle$ on f_0 is similar to that shown in Fig. 4. (b) The mean maximum tether length as a function of v for various dimensionless pulling device stiffnesses μ .

Both constant force load rate and constant pulling speed protocols give qualitatively similar tether extraction probabilities and maximum delamination forces f_c^{\max} . This is not surprising since in the two protocols are physically equivalent in both the infinitely stiff and infinitely soft pulling device limits, prior to delamination. In the large $\mu \propto K$ limit, a constant pulling speed forces the ligand to have the trajectory $x(t) = Vt$. Because we assume a linear force-extension relationship before delamination, this protocol is equivalent to a high constant force loading rate of $\Gamma \approx KV$ (or $\gamma \approx \mu v$). In the extremely soft pulling device limit, the elastic pulling device absorbs most of the extension and the force at which it acts on the ligand also increases linearly in time: $\Gamma \approx F_c V/x_0$ (or $\gamma \approx v f_c$).

However, we do find a qualitative difference in the mean tether length extracted, due to difference in the post-delamination forces between the two protocols. As functions of load rate and pulling speed, the maximum mean tether lengths attainable via linear force ramp are typically less than half of those achieved through constant pulling speed, all else being equal. This feature can be understood by considering how the receptor displacement, $x(t)$ and the ligand dissociation rate, $k_r(t)$ depend on time in each case. When the pulling speed is constant, after the tether forms, $x(t)$ increases linearly in time, and $k_r(t)$ is constant. When we apply a force ramp to the system, $x(t)$ increases quadratically in time once tether formation occurs. This would seem to imply longer tethers under the force ramp protocol; however, in this case, the dissociation rate $k_r(t)$ also increases exponentially in time. Thus, ligand detachment is much faster in the force ramp case, resulting in shorter observed mean tether lengths.

4. Summary and Conclusions

We modeled membrane-cytoskeleton delamination in series with a ligand-receptor bond and a deformable pulling device and determined the parameter regimes within which lipid tether extrusion is likely. Results from our model can be directly used to propose and analyse experiments in which cell or lipid vesicle membranes are pulled by

a breakable bond. For example, in [11], tethers are pulled from endothelial cells when large force barriers are overcome, but detachment of the pulling device from the tether is not considered. Performing such experiments with breakable ligand-receptor binds would provide the necessary data with which to test our predictions on the likelihood of tether formation and on the differences between fixed load rate and pulling speed protocols.

For both linear force ramp and constant pulling speed protocols, we find a wide window of ramp rates and pulling speeds that likely lead to tether extraction. However, we also find critical values of a dimensionless membrane-cytoskeleton delamination force, and a dimensionless spontaneous ligand-receptor dissociation rate beyond which tether formation is unlikely, regardless of all other parameters. We assumed in all of our analysis that the tether force-extension curve can be derived from local interactions with a Helfrich free-energy model. Finite-size membrane reservoirs and nonlocal energies such as area-difference elasticity would give rise to increasing forces as the tether is extended, thereby increasing the probability of ligand-receptor dissociation, and decreasing expected tether lengths $\langle X^* \rangle$.

Both linear force ramp and constant pulling speed protocols yield intermediate tether formation regimes, with a specific pulling speed v and specific linear ramp rate γ that maximizes the mean tether length $\langle X^* \rangle$ in the respective protocol. However, they present different tether dynamics after delamination leading to different expected tether lengths $\langle x^* \rangle$. Using both protocols, and our results, it may be possible to characterize membrane-cytoskeleton properties, provided sufficient information about the ligand-receptor binding energy and pulling device response are known. In general, such inverse problems are very ill-posed, but restricting the force-extension relationship to simple forms as we have done, one may be able to use the onset of tether formation as a way to estimate force parameters (such as F_0 , F_c and x_0).

While we have framed our analysis in terms of AFM experiments in which the strength of a ligand-receptor bond is probed while the receptor is in the membrane of a live cell, our basic model is relevant to leukocyte rolling as well. In leukocyte rolling, a bond between protein on a leukocyte microvilli and a protein in the membrane of an endothelial cell becomes stressed. Because the microvilli act like Hookean springs when pulled [3], and simultaneous extension of microvilli and tether extraction from the endothelial cells has been observed [4], our analysis is directly applicable to this system, with the cantilever replaced with a microvilli.

Finally, we note that we have treated the ligand-receptor bond rupturing as a stochastic Poisson process, while the deformation of membrane and cytoskeleton was considered deterministic. This approximation is good as long as $x_0 \gg d$. However, if the experiment is repeated, each region of membrane may have highly variable attachments to the cytoskeleton. In this case, a distribution of delamination forces F_c should be considered. Another source of stochasticity may arise when multiple adhesion points are being pulled, possibly leading to multiple tethers [36]. If the entire system is treated as a single, effective tether, the force-extension of this super-tether will rely on the statistics of how many individual tethers are still attached during the dynamics.

Acknowledgments

This work was supported by the NSF through Grant no. DMS-0349195 and by the NIH through Grant no. K25 AI058672.

- [1] H. Lodish, A. Berk, P. Matsudaira, C. A. Kaiser, M. Krieger, M. P. Scott, S. L. Zipursky, and J. Darnell. *Molecular Cell Biology*. W. H. Freeman and Company, 2003.
- [2] C. B. Korn and U. S. Schwarz. Dynamic states of cells adhering in shear flow: from slipping to rolling. *Phys. Rev. E*, 77:041904, 2008.
- [3] J. Y. Shao, H. P. Ting-Beall, and R. M. Hochmuth. Static and dynamic lengths of neutrophil microvilli. *Proceedings of the National Academy of Sciences of the United States of America*, 95(12):6797–6802, 1998.
- [4] G. Girdhar and J. Y. Shao. Simultaneous tether extraction from endothelial cells and leukocytes: Observation, mechanics, and significance. *Biophys. J.*, 93(11):4041–4052, 2007.
- [5] K. Schumacher, A. S. Popel, B. Anvari, W. E. Brownell, and A. A. Spector. Computational analysis of the tether-pulling experiment to probe plasma membrane-cytoskeleton interaction in cells. *Phys. Rev. E*, 80:041905, 2009.
- [6] R. M. Hochmuth and E. Evans. Extensional flow of erythrocyte membrane from cell body to elastic tether. *Biophys. J.*, 39:71–81, 1982.
- [7] J. Dai and M. P. Sheetz. Mechanical properties of neuronal growth cone membranes studied by tether formation with laser optical tweezers. *Biophys. J.*, 68(3):988–996, 1995.
- [8] D. Fygenon, J. F. Marko, and A. Libchaber. Mechanics of microtubule-based membrane extension. *Phys. Rev. Lett.*, 79:4497–4500, 1997.
- [9] T. R. Powers, G. Huber, and R. E. Goldstein. Fluid-membrane tethers: Minimal surfaces and elastic boundary layers. *Phys. Rev. E*, 65:041901, 2002.
- [10] I. Derényi, F. Julicher, and J. Prost. Formation and interaction of membrane tubes. *Phys. Rev. Lett.*, 88:238101, 2002.
- [11] M. Sun, J. S. Graham, B. Hegedus, F. Marga, Y. Zhang, G. Forgacs, and M. Grandbois. Multiple membrane tethers probed by atomic force microscopy. *Biophys. J.*, 89(6):4320–4329, 2005.
- [12] G. Koster, A. Cacciuto, I. Deréyi, D. Frenkel, and M. Dogterom. Force barriers for membrane tube formation. *Phys. Rev. Lett.*, 94:068101, 2005.
- [13] D. Cuvelier, N. Chiaruttini, P. Bassereau, and P. Nassoy. Pulling long tubes from firmly adhered vesicles. *Europhys. Lett.*, 71:1015–1021, 2005.
- [14] M. Benoit, D. Gabriel, G. Grerisch, and H. E. Gaub. Discrete interactions in cell adhesion measured by single-molecule force spectroscopy. *Nature Cell Biol.*, 2:313–317, 2000.
- [15] Ana-Suncana Smith, E. Sackmann, and U. Seifert. Pulling tethers from adhered vesicles. *Phys. Rev. Lett.*, 92:208101, 2004.
- [16] E. Glassinger and R. M. Raphael. Influence of thermally driven surface undulations on tethers formed from bilayer membranes. *Biophys. J.*, 91:619–625, 2006.
- [17] R. M. Raphael and R. E. Waugh. Accelerated interleaflet transport of phosphatidylcholine molecules in membranes under deformation. *Biophys. J.*, 71:1374–1388, 1996.
- [18] F. M. Hochmuth, J. Y. Shao, J. Dai, and M. P. Sheetz. Deformation and flow of membrane into tethers extracted from neuronal growth cones. *Biophys. J.*, 70:358–369, 1996.
- [19] R. Merkel, P. Nassoy, A. Leung, K. Ritchie, and E. Evans. Energy landscapes of receptor-ligand bonds explored with dynamic force spectroscopy. *Nature*, 397:50–53, 1999.
- [20] E. Evans. Probing the relation between force-lifetime and chemistry in single molecular bonds. *Ann. Rev. Biophys. Biomol. Struct.*, 30:105–128, 2001.
- [21] B. Heymann and H. Grubmüller. Dynamic force spectroscopy of molecular adhesion bonds. *Phys. Rev. Lett.*, 84:6126–6129, 2000.
- [22] O. K. Dudko, A. E. Filippov, J. Klafter, and M. Urbakh. Beyond the conventional description of dynamic force spectroscopy of adhesion bonds. *Proceedings of the National Academy of Sciences of the United States of America*, 100(20):11378–11381, 2003.
- [23] W. Hanley, O. McCarty, S. Jadhav, Y. Tseng, D. Wirtz, and K. Konstantopoulos. Single molecule characterization of p-selectin/ligand binding. *J. Biol. Chem.*, 278:10556–10561, 2003.
- [24] J. Schmitz, M. Benoit, and K. E. Gottschalk. The viscoelasticity of membrane tethers and its importance for cell adhesion. *Biophys. J.*, 95:1448–1459, 2008.
- [25] L. Miao, U. Seifert, M. Wortis, and H. G. Döbereiner. Budding transitions of fluid-bilayer vesicles: the effect of area-difference elasticity. *Phys. Rev. E*, 49:5389–5407, 1994.
- [26] R. Afri and A. Ikai. Force profiles of protein pulling with or without cytoskeletal links studied

- by afm. *Biophys. Biochem. Res. Comm.*, 348:238–244, 2006.
- [27] N. Borghi and F. Brochard-Wyart. Tether extrusion from red blood cell: Integral proteins unbinding from cytoskeleton. *Biophys J.*, 93:1369–1379, 2007.
- [28] G. I. Bell. Models for the specific adhesion of cells to cells. *Science*, 200:618–627, 1978.
- [29] E. Evans and K. Ritchie. Dynamic strength of molecular adhesion bonds. *Biophys. J.*, 72:1541–1555, 1997.
- [30] E. B. Walton, S. Lee, and K. J. Van Vliet. Extending bell’s model: How force transducer stiffness alters measured unbinding forces and kinetics of molecular complexes. *Biophys. J.*, 94:2621–2630, 2008.
- [31] D. Leckband, W. Müller, F.-J. Schmitt, and H. Ringsdorf. Molecular mechanisms determining the strength of receptor-mediated intermembrane adhesion. *Biophys J.*, 69:1162–1169, 1995.
- [32] Y. Sako, A. Nagafuchi, S. Tsukita, M. Takeichi, and A. Kusumi. Cytoplasmic regulation of the movement of e-cadherin on the free cell surface as studied by optical tweezers and single particle tracking: Coralling and tethering by the membrane cytoskeleton. *J. Cell Biol.*, 140:1227–1240, 1998.
- [33] M. D. Ward, M. Dembo, and D. A. Hammer. Kinetics of cell detachment: Effect of ligand density. *Annals of Biomedical Engineering*, 23:322–331, 1995.
- [34] C. E. Morris and U. Homann. Cell surface area regulation and membrane tension. *J. Membrane Biol.*, 179:79–102, 2001.
- [35] E. Evans and W. Rawicz. Entropy-driven tension and bending elasticity in condensed-fluid membranes. *Phys. Rev. Lett.*, 64:2094–2097, 1990.
- [36] O. Björnham and O. Axner. Multipili attachment of bacteria with helix-like pili exposed to stress. *J. Chem. Phys.*, 130:235102, 2009.